International Journal of Mass Spectrometry 302 (2011) 12–18

Contents lists available at ScienceDirect

International Journal of Mass Spectrometry

journal homepage: www.elsevier.com/locate/ijms

Hydrogen/deuterium exchange mass spectrometry for characterizing phosphoenolpyruvate-induced structural transitions in *Mycobacterium tuberculosis* 5-enolpyruvylshikimate-3-phosphate synthase (EC 2.5.1.1)

Alessandra Vaso[a], Diógenes S. dos Santos[b], Luis Augusto Basso[b], Mario S. Palma[a,*]

[a] Laboratory of Structural Biology and Zoochemistry, CEIS/Department of Biology, Institute of Biosciences, UNESP, Rio Claro, SP 13506-900, Brazil
[b] Centro de Pesquisas em Biologia Molecular e Funcional/PUCRS. Avenida Ipiranga 6681, Tecnopuc, Partenon 90619-900, Porto Alegre, RS, Brazil

ARTICLE INFO

Article history:
Received 22 March 2010
Received in revised form 25 May 2010
Accepted 2 June 2010
Available online 11 June 2010

Keywords:
ESI-MS
H/D exchange
Mass spectrometry
Proteins dynamics
Shikimate pathway

ABSTRACT

The enzyme 5-enolpyruvylshikimate-3-phosphate synthase (EPSPS) catalyzes the reaction between shikimate-3-phosphate (S3P) and phosphoenolpyruvate (PEP) to form 5-enolpyruvylshikimate-3-phosphate, an intermediate in the shikimate pathway, which leads to the biosynthesis of aromatic amino acids. The two-domain structure of EPSPS is formed by a 6-fold replication of protein folding units, each one formed by two parallel α-helices and four-stranded β-sheets. The apo form of the enzyme exists in an open conformation, but when bound to PEP, the EPSPS conformation is closed. The H/D exchange properties of EPSPS from *Mycobacterium tuberculosis* (*Mt*) were studied for both enzyme conformations using ESI-mass spectrometry. We mapped the identified H/D exchange sites on the 3D structure. H/D exchange revealed that the enzyme undergoes extensive conformational change upon forming the PEP complex, which seem to favor solvent access at domain 1, while they partially prevent solvent access to domain 2. This may be part of the catalysis mechanism of the enzyme, stabilizing S3P binding and inducing cleft closure, which controls the entrance of substrate molecules.

© 2010 Elsevier B.V. All rights reserved.

1. Introduction

Tuberculosis was declared a global epidemic, and it is a public health concern due to its multidrug resistance (MDR) [1]. The treatment of active cases of tuberculosis is a serious problem for chemotherapy, as it requires a simultaneous use of two or more frontline drugs, such as isoniazid, ethambutol, rifampicin and streptomycin [2]. Recent outbreaks of tuberculosis caused the emergence of MDR strains, mainly in HIV- infected individuals. Outbreak of these strains attracted the attention of global programs on new drug development, working toward selective inhibition of enzymes from the resistant *M. tuberculosis* strains [3]. Despite the huge efforts by academic institutions and pharmaceutical companies, the small number of target macromolecules limits progress toward development of novel drugs.

The shikimate pathway synthesizes aromatic amino acids, p-aminobenzoic acid and other essential metabolites, such as ubiquinone, menaquinone, and vitamin K. In a sequence of seven metabolic steps, phosphoenolpyruvate and erythrose 4-phosphate are converted to chorismate, the precursor for aromatic amino acids and many aromatic secondary metabolites. The shikimate pathway links the metabolism of carbohydrates to the biosynthesis of aromatic compounds. The enzymes in the shikimate pathway are attractive targets for the development of novel herbicides and antimicrobial drugs, as this pathway is essential in algae, higher plants, bacteria and fungi, but it is absent in mammals [4,5].

The indispensability of the mycobacterial shikimate pathway and its absence from the human host indicate that the enzyme components for this metabolic route are promising targets for developing novel, non-toxic agents against human pathogens [6]. The sixth reaction step of this pathway is characterized by transfer of an enolpyruvyl moiety from PEP to S3P, followed by elimination of inorganic phosphate with consequent formation of 5-enolpyruvylshikimate 3-phosphate (EPSP); this step is catalyzed by EPSPS [7].

EPSPS enzymes are classified into two distinct classes: class I—naturally found in plants and many bacteria and sensitive to the inhibitor glyphosate; and class II—occurs naturally in glyphosate-tolerant organisms and relatively resistant to glyphosate inhibition [7,8]. Notably, *Mt*EPSPS is a class I enzyme [9].

EPSPS is a monomeric enzyme with a molecular mass around 46 kDa. X-ray crystal structures from different bacteria indicate that it has two domains, with the active site near the interdomain crossover segment [7]. The apo form exhibits an open conformation, however, binding to a substrate/inhibitor alters the conformation to a closed form [9] (Fig. 1A′ and B′). Each domain

* Corresponding author. Tel.: +55 19 3526 4163; fax: +55 19 3526 4163.
E-mail address: mspalma@rc.unesp.br (M.S. Palma).

1387-3806/$ – see front matter © 2010 Elsevier B.V. All rights reserved.
doi:10.1016/j.ijms.2010.06.002

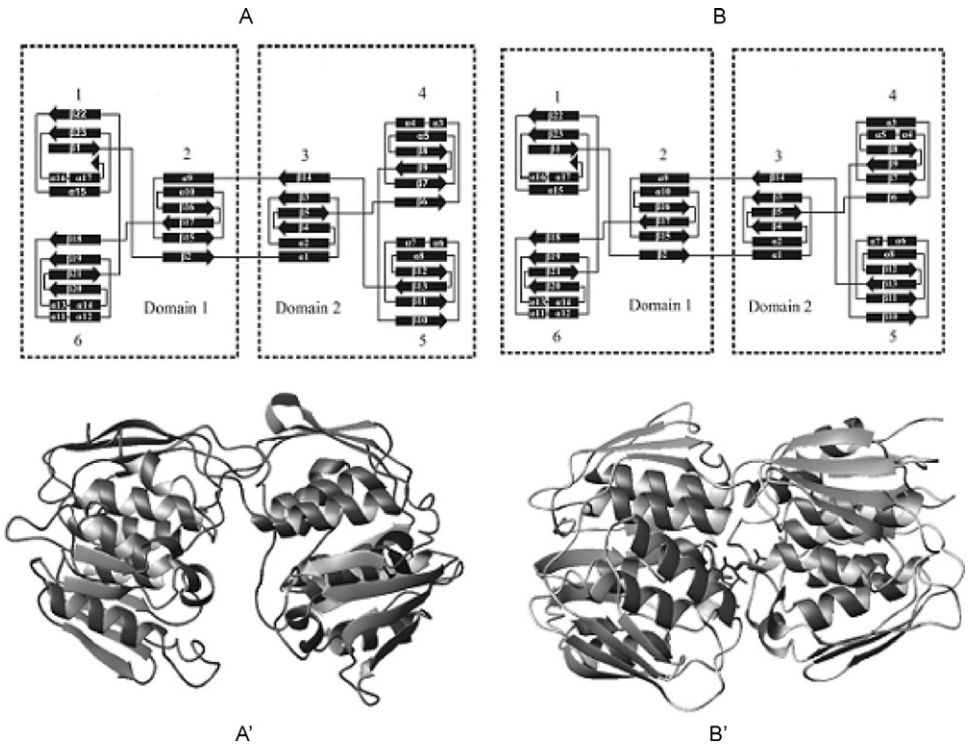

Fig. 1. Illustrations of the chain tracing of *Mt*EPSPS and the order of the secondary structural elements, as they occur in the enzyme molecule, both for the apo form (A) and the PEP-bound form of the enzyme (B). Both forms contain two domains (1 and 2). In the apo form, each domain is comprised of three copies of a βαβαββ-folding unit (A). The four-stranded β-sheet structures of each unit contain both parallel and antiparallel strands, while the helices are parallel. The two-domain structure of the apo form has a distinctive fold, which is formed by a 6-fold replication of the protein folding units, each one formed by two parallel α-helices and a four-stranded β-sheet (A). Domain 1 is comprised of the folding units 1, 2 and 6, while domain 2 is comprised of the folding units 3, 4 and 5. The representation for the PEP-bound form (B) reveals small structural rearrangements at unit 4, resulting from conformational changes induced by the PEP binding. The ribbon diagrams of the 3D structures for apo-*Mt*EPSP (PDB ID: 2BJB), known as the open form (A′), and for PEP-bound *Mt*EPSPS (PDB ID: 2O0E), known as the closed form (B′). The diagram indicates certain α-helices and β-strands.

is comprised of three copies of βαβαββ-folding units; the four-stranded β-sheet structures in each unit contain both parallel and antiparallel strands, while the helices are parallel (Fig. 1A and B). The two-domain structure of the apo form has a distinctive fold, characterized by a 6-fold replication of the protein folding units, each one formed by two parallel α-helices and four-stranded β-sheets. The structural units are related by an approximate 3-fold symmetry axis; in each domain, three of the helices are completely buried by a surface formed with the three β-sheets and the solvent accessible faces of the other helices [10].

The structure of apo-*Mt*EPSPS was determined by crystallography [11], while the structure of substrate-bound *Mt*EPSPS was modeled using structural bioinformatics tools [3]. The EPSPS domains are responsible for the dynamic motion between the open and closed conformations. In the apo form, the domains have an open conformation [12], while in the liganded form, which is bound to PEP/glyphosate, the domains are in a closed conformation [3] (Fig. 1A′ and B′). S3P binds EPSPS, but for entropic reasons, is unable to induce the domain closure alone [13]. In contrast, when glyphosate binds to the EPSPS–S3P complex, it induces protein reorganization with a loss in flexibility. Inhibition of glyphosate is competitive compared to PEP, as the inhibitor occupies a large part of the PEP-binding site, suggesting that binding of this substrate must induce domain closure [14]. However, the extent of the conformational change caused by PEP binding to the enzyme is unknown.

Typically, a specific conformation of a folded protein correlates to its biological activity [15]. The folding is strongly influenced by non-covalent interactions, such as hydrogen bonding, ionic interactions, van der Waals' forces and hydrophobic effects [16,17]. Proteins may fold and unfold constantly depending on the environmental conditions; intra and intermolecular bonding forces generally ensure a more populated conformation for the native state over other conformations [18].

Mass spectrometry is a widely used tool in studies of protein folding/unfolding to map structural changes associated with specific mutations, induced by both ligand and protein–protein interactions [18]. An array of MS-based methodologies, such as H/D exchange and limited proteolysis, which are associated with ESI-MS, are frequently used to probe both the structure and dynamics of individual proteins [19–21]. Presumably, the solvent can access flexible or dynamic regions of a protein more readily, and such events are reflected in the rate of deuterium exchange. Regions of limited flexibility may be less solvent accessible; however, slow deuterium exchange may also reflect high stability of hydrogen bonds [9].

Monitoring amide deuterium exchange by ESI-MS and MS/MS is an efficient experimental strategy for examining solvent accessibility in the protein backbone amide hydrogens. This method provides detailed information about the environment of distinct regions of the protein and how that environment is affected by ligand binding [22–25].

Mapping the conformational changes identified by H/D exchange on the 3D structure along the secondary structure of both *Mt*EPSPS conformations may contribute to a more complete understanding of this enzyme–substrate interaction. Notably, the EPSPS-PEP interactions may be influenced by induced-fit and even minor conformational changes may result in dramatic changes of enzyme activity [8]. Thus, to investigate these substrate-induced conformational changes, we report herein the H/D exchange properties of *Mt*EPSPS both for the apo and the PEP-bound forms of the enzyme. EPSPS enzymes have been considered an attractive target for the

development of antimicrobial drugs. Knowledge about their interaction with substrates and inhibitors will certainly contribute to a better understanding of their ligand-induced structural dynamics.

2. Experimental

2.1. Protein sample

The active, recombinant *Mt*EPSPS was expressed and purified as previously described [26,27]. The protein pellet from an 80% (w/v) ammonium sulfate solution was resolubilized and dialyzed exhaustively against 5 mM sodium phosphate, pH 6.9. The protein concentration was determined spectrophotometrically using the calculated extinction coefficient for the protein under native conditions and for the denatured protein [28].

2.2. H/D exchange, pepsin digestion and mass spectrometry

Protein samples were analyzed in reversed phase HPLC column, POROS 10R2 (100 mm × 0.25 mm; Perceptive Biosystems), using a flow rate of 255 nL/min; samples of the intact protein were eluted using an acetonitrile gradient from 5% to 85% (v/v) (containing 0.02% (v/v) TFA) over the course of 7 min, directly into the mass spectrometer ionization system.

The concentration of the *Mt*EPSPS stock solution was 1.5 mM in phosphate buffer (100 mM, pH 6.9, 25 °C). At a final concentration of 75 μM, the enzyme was labeled by diluting the solution 20-fold with D_2O (5 mM sodium phosphate, pD 6.9, 25 °C). When necessary, the enzyme, in the presence of PEP, was incubated in the medium described above at a final concentration of 3 mM. Solutions were maintained at 25 °C and the time of isotope exchange ranged from 1 min to 8 h. The pH and pD values reported were taken directly with a pH meter and were not corrected for isotope effects. At each time point, aliquots (20 μL, 30 nmol) were taken out of the exchange tube, quenched by mixing the solution with a 1:1 ratio of the quenching buffer (D_2O, 100 mM sodium phosphate, pD 2.5) and cooled to 0 °C to slow down the H/D exchange. Immediately after quenching, the exchanged *Mt*EPSPS aliquots were digested over 5 min at 0 °C by adding 1 μL of a precooled pepsin solution (1 mg/mL in 5% (v/v) formic acid). We then took aliquots (5 μL) from the digest and loaded them onto a microbore HPLC column (20 cm × 0.32 mm, 15 μm, LUNA C18) in an ice bath. The peptides were separated over 10 min using a 5–70% acetonitrile/water gradient (containing 0.05% (v/v) TFA). The column eluent (100 μL/min) was delivered directly to the mass spectrometer for ESI-MS and ESI-MS/MS experiments.

Using PEEK tubing (1/16 in. o.d. × 0.25 mm i.d.), the HPLC system was connected directly to the ESI probe of the mass spectrometer. A flow of 100 μL/min to the ESI probe was obtained by splitting the primary flow of 600 μL/min via a T-piece, allowing the compounds to be monitored and their molecular masses to be determined. The LC eluents were analyzed by positive electrospray ionization (ESI^+). The MS experiments were performed using an ESI triple quadrupole instrument, model Quatro II (Micromass, UK), in the continuous acquisition mode; a capillary voltage of 3.5 kV, a cone voltage of 30 V, and a desolvation gas temperature of 80 °C was used. The masses were calibrated with intact horse heart myoglobin, and its typical cone voltage induced fragments. The ESI spectra were obtained in the continuous acquisition mode, scanning from m/z 100–2500 with a scan time of 5 s. The spectral data were acquired and monitored using the MassLynx software (Micromass).

Peptides were sequenced using ESI^+-MS/MS under the LC conditions described above. Typical conditions were a capillary voltage of 3 kV, a cone voltage of 30 V, a collision gas pressure of 3.5×10^{-3} mbar, and a desolvation gas temperature of 80 °C. The singly charged protonated molecules of the precursors were selected in Q1 and subjected to collision-induced dissociation (CID) with argon gas at a collision energy of 52 eV; the product ions were detected by scanning Q3. All of the MS/MS data were acquired in the continuous acquisition mode, scanning from m/z 40 to the m/z value of the $[M+H]^+$ ion of each peptide, with a scan time of 5 s. The spectral data were acquired and monitored using the MassLynx software. Peptide sequences were assigned manually from the ESI^+-MS/MS product ion mass spectra, aided by MaxEnt1 software (Micromass, UK). Mass spectrometry analysis for all the samples in each comparison set were done on the same day, using the same instrumental conditions. Deconvolution of the intact protein spectra was performed with the program Transform (Waters). The error for each data point in the intact protein was 0.3 Da (based on multiple measurements).

As the proteolysis solvents were used in the HPLC protocols, the labile deuterons in both the side chains and the N- and C-terminal ends were replaced by protons. Deuterium back exchange at amide linkages was minimized by cooling the chromatographic system to 0 °C, maintaining a pH of 2.5, and using a steep elution gradient. Three control samples were analyzed under the same conditions to assess the extent of exchange that occurs during analysis, despite the quenching conditions. The results from these control samples, the undeuterated protein ($m_{0\%}$), and the entirely exchanged protein ($m_{100\%}$) were used to adjust for artificial exchange that occurred during analysis as previously described [29]. The undeuterated control sample was prepared by diluting a solution of *Mt*EPSPS into D_2O buffer under quenching conditions (0 °C at pH 2.5).

The mass of each peptide was taken as the centroid of the isotopic envelope using the program MassLynx (Micromass, UK). An experimental correction is necessary to account for the exchange of deuterium during HPLC (back exchange) and the use of a 20-fold excess of D_2O during the labeling step, which limits the forward exchange reaction. In our experiments, a 100% deuterated protein control was prepared by diluting the protein stock in the labeling solution and quenching buffer, incubating at 50 °C for 8 h and then incubating at room temperature (approximately 25 °C) for 24 h.

The data were processed using the centroid isotopic distributions corresponding to the +1 charge state of each deuterated peptide. The corrected level of deuterium incorporation was calculated according to the following Eq. (1) [29,30]:

$$D = \frac{m - m_{0\%}}{m - m_{100\%}} \times N \quad (1)$$

where: D is the number of amide hydrogen atoms incorporated in a specific peptide; m is the experimental centroid mass of the deuterated peptide at a certain time point; $m_{0\%}$ is the centroid mass of the undeuterated peptide; $m_{100\%}$ is the centroid mass of the 100% deuterated control peptide; N is the number of amide hydrogens for each peptide characterized.

Thus, the deuterium level (D) at any peptic fragment amide linkage during the time course of incubation in presence of D_2O is given by the following Eq. (2) [31]:

$$D = N - N_{ex}\, e^{-k.t} \quad (2)$$

where: N_{ex} is the number of exchanging amide hydrogen atoms; k corresponds to the respective exchange rate constants for the exchanging amide hydrogen atoms; t is the specific time of enzyme incubation in presence of D_2O.

Adjustments for a small amount of deuterium loss during digestion and HPLC protocols were made using results obtained for each of the control samples as described above. This artificial loss of deuterium was 11–13% in most peptides.

2.3. Molecular models

A molecular model for *Mt*EPSPS was utilized to map the positions that underwent conformational change under the experimental conditions described above. The open conformation model, characteristic of the apo form of the enzyme, was generated using the atomic coordinates from 2BJB [http://www.rcsb.org/pdb/explore.do?structureId=2BJB]. The closed conformation model, characteristic of the substrate-bound form, was the same as previously reported in Protein Data Bank (PDB 2OOE) (http://www.pdb.org/pdb/explore/explore.do?structureId=2O0E). Briefly, for modeling the EPSP synthase, we used restraint-based modeling, implemented using the program PARMODEL [34] The closed conformation model was generated using the α-carbon atomic coordinates from 2O0E (http://www.rcsb.org/pdb/explore/explore.do?structureId=2O0E). The atomic coordinates of all water molecules were removed from the EPSPS structure. The S3P and PEP of the template protein were kept in the structure for the closed conformation. Finally, the model was obtained by optimizing the objective function in Cartesian space. The optimization was carried out

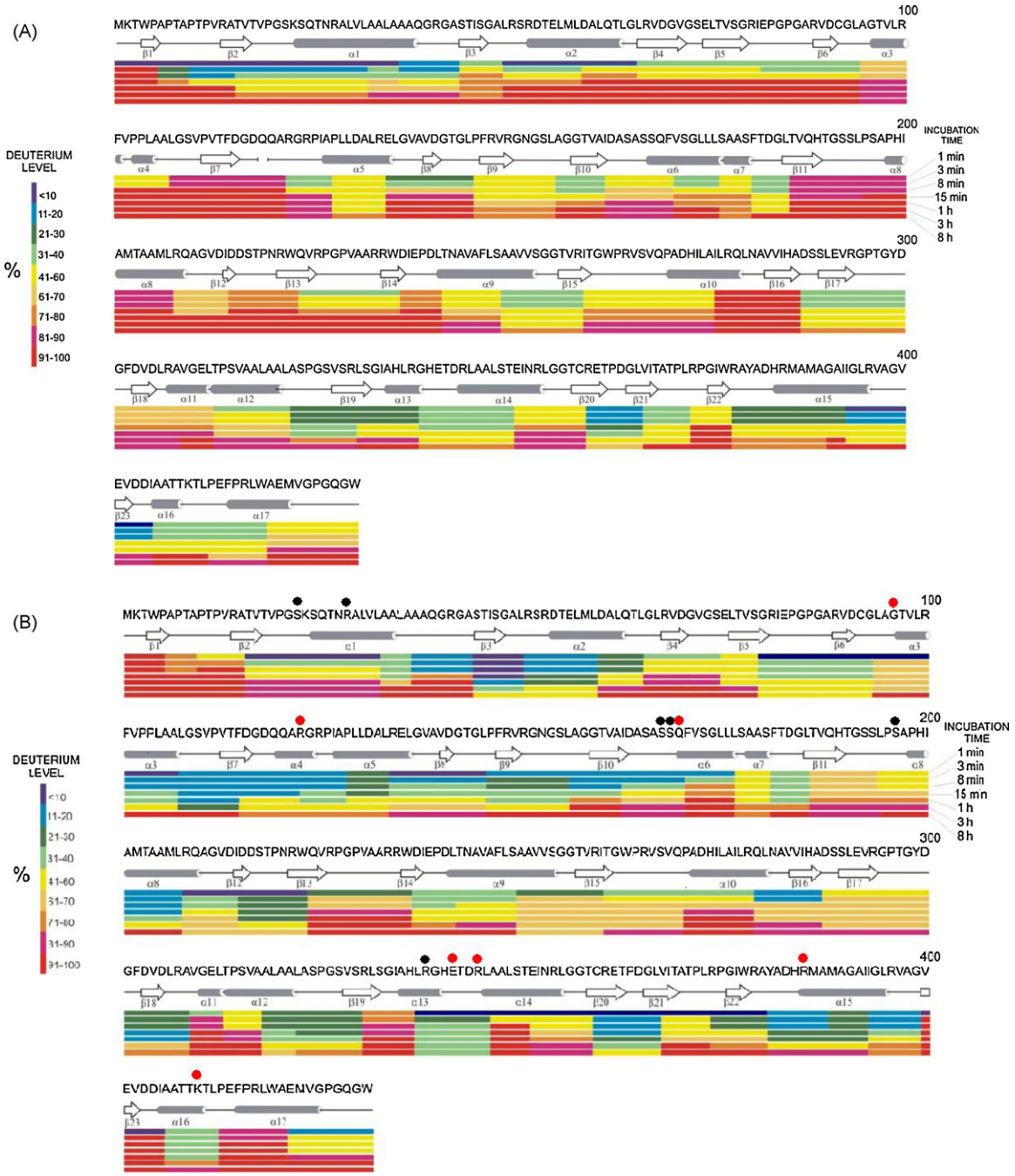

Fig. 2. Schematic representation of the relative deuterium incorporation in each peptic fragment from different regions of the *Mt*EPSPS, both for the apo (A) and PEP-bound (B) forms of the enzyme. The scheme shows the primary sequence of the enzyme, the secondary structure elements in each enzyme's conformation, and a series of colored bars below the sequence represent, in descending order, deuterium uptake at 1 min, 3 min, 8 min, 15 min, 1 h, 3 h, and 8 h. The dark blue color represents the lowest level of deuterium incorporation, and a gradient of different colors shifting in direction to the red represents the increasing deuterium incorporation, where red represents the highest level of deuterium incorporation. α-Helices are represented as cylinders, while *β*-strands are represented as arrows. The residues at the S3P and PEP binding sites are indicated with black and red spots, respectively.

via the variable target function method, employing the conjugate method [35]. Several slightly different models can be calculated by varying the initial structure. A total of 1500 models were generated for each EPSPS conformation state, and the final models were selected based on stereochemical quality. All model processing was performed on a Beowulf cluster, with 14 nodes (B16/AMD Athlon 1800+; BioComp, Rio Claro, SP, Brazil).

3. Results and discussion

Structural changes enabling isotope exchange may involve global unfolding or minor fluctuations that allow exchange at individual amide linkages. The objective of this investigation was to determine the regions most accessible to the solvent, i.e., to identify and to map the sequences susceptible to conformational change on the *Mt*EPSPS 3D structure, including both spontaneous structural changes in the apo form of the enzyme as well as those induced by PEP binding.

3.1. The global H/D exchange of MtEPSPS

ESI-MS analysis of apo-*Mt*EPSPS revealed a molecular mass of 46427.8 Da, which fits well with the predicted value of 46427.7 Da. As deuterium labeling occurs when the protein is in its native state, the amount of deuteration reflects solvent accessibility at certain protein regions. Following H/D exchange, the global mass changes in the apo-*Mt*EPSPS and the *Mt*EPSPS-PEP complex were determined by analyzing the intact protein by LC–ESI-MS (not shown results). *Mt*EPSPS is comprised of 450 amino acids. Considering the presence of 33 proline residues (which do not contribute with amide hydrogens) and that the C- and N-terminal deuterons are removed by back-exchange with the quenching solution, the maximum number of exchangeable amide hydrogens in this protein is 415. After an 8-h incubation, the enzyme incorporated 375 deuterons into the apo form and 363 into the PEP-bound form (already corrected for back-exchange), which corresponds to 90% and 87%, respectively, of the total amide hydrogens. Apparently, the PEP complex partially prevents solvent access to a series of amino acid residues.

3.2. The localized H/D exchange and conformational change in MtEPSPS

Initially, it should be emphasized that a comparison between the molecular models for the open and closed enzyme conformations (Fig. 1A′ and B′) reveals that the secondary structure of both enzyme forms are slightly different from each other. This indicates that *Mt*EPSPS undergoes certain structural rearrangements after PEP binding. Apo-*Mt*EPSPS has two large domains. Domain 1 is comprised of the units 1, 2, and 6, while domain 2 contains the units 3, 4 and 5; all of the units are βαβαββ-folds (Fig. 1A). This folding pattern was slightly modified by PEP binding; units 1, 2, 3, and 5 maintained the βαβαββ-fold, while units 4 and 6 presented a βαβαβα-fold (Fig. 1B). The protein was completely mapped using LC–ESI-MS and collision-induced dissociation (CID) of the proteolytic fragments. The level of deuterium incorporated in the protein backbone, both in the apo and PEP-bound forms, were probed by mass analysis of the peptic fragments at various time points. These results were used to locate specific differences in deuterium incorporation between the apo form and the PEP-liganded form. Digestion of *Mt*EPSPS with pepsin produced 67 peptic fragments, which covered 98% of the protein sequence (see Figure S1 in the Supplement information).

Fig. 2 shows the primary sequence of *Mt*EPSPS, its secondary structure, and a color coded representation of the deuterium incorporation in both forms of *Mt*EPSPS at different incubation times. Comparison of the deuterium exchange percentages between the apo (Fig. 2A) and PEP-bound forms (Fig. 2B) as a function of time (1 min, 3 min, 8 min, 15 min, 1 h, 3 h, and 8 h) reveals many differences between the open and closed states for *Mt*EPSPS.

The H/D exchange rate constants were determined for a group of 22 peptic fragments, shown in Table 1, for both the apo and PEP-bound forms of the enzyme. These peptides were selected because they are representative of regions structurally important to *Mt*EPSPS molecule, especially for those regions containing residues at the binding site. A general comparison of the data in Table 1 reveals that 80 exchanging hydrogens (N_{ex}) were observed in this group of peptides from apo-*Mt*EPSPS, while only 22 deuterons were observed in PEP-bound *Mt*EPSPS. This reflects a strong protective effect from PEP binding on solvent accessibility to the amide hydrogens.

Table 1
Constants of H/D exchange calculated according to Eq. (2) and number of amide hydrogens exchanged in the backbone of the Apo-*Mt*EPSPS and PEP-*Mt*EPSPS complex for enzyme incubated during 1 min at 25 °C in the presence of D_2O.

Residues	Apo-*Mt*EPSPS		PEP-*Mt*EPSP complex	
	N_{ex}	k (min^{-1})	N_{ex}	k (min^{-1})
5–9	3.20 ± 0.55	2.00 ± 0.40	3.15 ± 0.35	1.96 ± 0.25
16–32	3.10 ± 0.60	1.87 ± 0.35	3.90 ± 0.50	2.44 ± 0.35
63–67	2.00 ± 0.45	1.25 ± 0.25	–	–
83–94	4.30 ± 0.80	2.70 ± 0.45	3.40 ± 0.60	2.10 ± 0.40
95–101	3.90 ± 0.75	2.45 ± 0.50	–	–
122–127	3.30 ± 0.60	2.06 ± 0.40	–	–
146–155	5.10 ± 0.95	3.19 ± 0.65	–	–
163–170	3.70 ± 0.65	2.31 ± 0.45	–	–
171–176	2.40 ± 0.50	1.51 ± 0.30	–	–
208–214	4.30 ± 0.85	2.69 ± 0.55	–	–
269–279	5.10 ± 1.05	3.20 ± 0.60	–	–
281–287	4.70 ± 0.90	2.94 ± 0.55	–	–
300–308	5.10 ± 1.10	3.19 ± 0.60	2.20 ± 0.40	1.38 ± 0.25
309–317	4.90 ± 0.90	3.06 ± 0.55	2.80 ± 0.75	1.75 ± 0.47
313–319	2.00 ± 0.35	1.25 ± 0.25	2.90 ± 0.55	1.81 ± 0.35
322–331	5.20 ± 1.15	3.25 ± 0.60	1.90 ± 0.47	1.18 ± 0.30
341–349	2.80 ± 0.55	1.75 ± 0.35	–	–
367–373	2.20 ± 0.40	1.38 ± 0.25	–	–
382–389	4.10 ± 0.80	2.57 ± 0.50	–	–
393–398	1.90 ± 0.35	1.19 ± 0.25	–	–
406–412	3.20 ± 0.65	2.00 ± 0.40	2.00 ± 0.65	1.25 ± 0.40
420–429	3.70 ± 0.70	2.31 ± 0.40	–	–

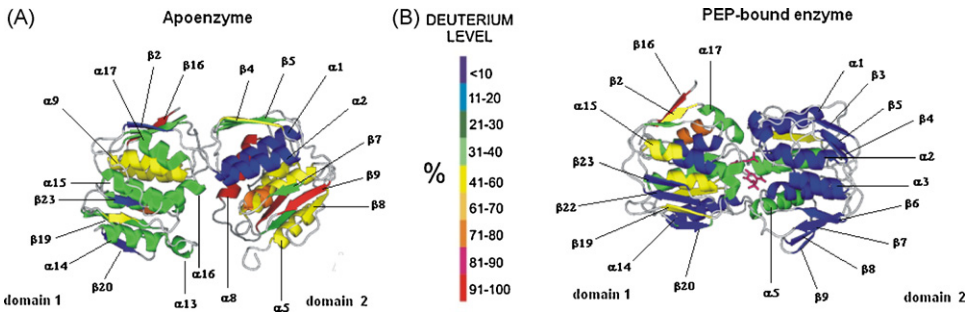

Fig. 3. Ribbon diagram of the three-dimensional structure of apo-*Mt*EPSP (A) and of the PEP-bound *Mt*EPSPS (B), after 1-min incubation in presence of D_2O, using a color code to indicate deuterium incorporation in the protein.

A comparison between the *Mt*EPSPS model with that obtained for *E. coli* EPSPS [14] suggests that the amino acid residues participating in the substrate binding sites for S3P are as follows: Ser^{22}, Arg^{28}, Ser^{167}, Ser^{168}, Ser^{196}, and Arg^{338} (their positions are indicated with black spots in Fig. 2B). Furthermore, those residues constituting the binding site for PEP are as follows: Gly^{96}, Arg^{124}, Gln^{169}, Glu^{341}, Arg^{344}, Arg^{385} and Lys ^{410} (their positions are indicated with red spots in Fig. 2B). A careful comparative analysis of Fig. 2A and B reveals that the peptic fragments containing the residues at the PEP binding site (fragments 95–101, 122–127, 163–170, 341–349 and 382–389) became less susceptible to H/D exchange after PEP binding. The results of Table 1 indicate that these regions probably became more rigid and less solvent accessible (fragments 300–308, 309–317, 322–331 and 406–412) or even completely inaccessible (fragments 63–67, 95–101, 122–127, 146–155, 163–170, 171–176, 208–214, 269–279, 281–287, 341–349, 367–373, 382–389, 393–398 and 420–429). It must be emphasized that the fragment 16–32, despite to be localized close to the N-terminal region of the molecule, is relatively protected from the solvent access both in the apo and in the PEP-complexed enzyme. The rate constants of H/D exchange reported in Table 1 are the same order of magnitude as those generally observed for peptides that are fully solvent accessible [32,33]. Considering the fragments shown in Table 1, the number of exchanging hydrogens in the apo-*Mt*EPSPS decreased from 80 to 22 in the enzyme complexed to PEP, suggesting that the secondary structure of the enzyme became more stable due to PEP complex formation.

Fig. 3 shows the 3D structure of *Mt*EPSPS in a ribbon representation, after 1 min incubation in presence of D_2O, for both the apo (Fig. 3A) and PEP-bound forms of the enzyme (Fig. 3B), using a color code to indicate deuterium incorporation in the protein. Fig. 3A clearly shows that in the apo form helices-α1 and 2 as well as β-sheets 2, 20 and 23 were the only solvent inaccessible elements of the secondary structure. In contrast, Fig. 3B shows that after PEP binds to the enzyme, the elements of secondary structure that became solvent inaccessible are α-helices 1, 2, 14, 20 and 21 as well as β-sheets 3, 6, 12, 13, 20 and 21. These results suggest that PEP binding induces a series of conformational changes in *Mt*EPSPS, making the enzyme more compact, especially for domain 2.

It has been reported that, as a general rule, the apo form adopts an open conformation, in which the regions containing the binding site residues contain large areas of solvent accessibility that are stably maintained by a reduced number of hydrogen bonds [3,12,13]. However, the binding of PEP to the enzyme induces a conformation change to a closed form such that the binding site regions of the enzyme become more compact.

4. Conclusions

The results above suggest that *Mt*EPSPS undergoes extensive conformational change when it complexes with PEP, changing from the open to the closed conformation. If these observations are correlated with the reduced level of H/D exchange presented by the ligand-bound form compared to the apo form, it is possible to speculate that the more compact conformation may be associated with the rearrangement of the secondary structure after PEP binding. The enzyme's flexibility may be part of a mechanism for rapid interconversion between different conformations of this protein by rearranging its secondary structure [9]. If the apo-EPSPS molecules were too stable, they could not make a quick transition from the open form to the closed form.

*Mt*EPSPS undergoes a series of PEP-induced conformational changes, which probably result in synergistic effects that favor solvent access to the core of the molecule in domain 1 but also prevent solvent access, especially in domain 2. The binding of S3P alone to EPSPS does not induce the domains' closure [22]; however, the results of the present investigation clearly demonstrate that the binding of PEP caused the domains to close. Recently, it was reported that binding of glyphosate to the enzyme also induces domain closure, extensive conformational change, and protein reorganization [9].

It is important to emphasize that the binding of S3P to the enzyme requires three molecules of water to stabilize the first substrate in its binding site [13]. Thus, it is likely that the binding of PEP compacts domain 2, preventing the access of the solvent to its core, while it favors the solvent access to domain 1. Furthermore, the PEP-induced conformational change in the *Mt*EPSPS molecule may be part of a mechanism that both favors hydration of the substrate binding site in the domain 1 and induces the cleft closure after substrate binding, beginning the catalysis.

The monitoring of amide H/D exchange with ESI-mass spectrometry applied to full-length *Mt*EPSPS in the apo- and PEP-bound states has demonstrated the solution dynamics of the enzyme and the conformational change induced upon binding one of its substrates. This experimental approach took into account differences in peptide masses with differential time exposures to the solvent containing D_2O. Our approach permitted us to analyze the enzyme under two different conformations. Using the *Mt*EPSPS 3D model, we mapped the structural information from the H/D exchange and ESI-mass spectrometry experiments, which permitted us to identify certain structural elements important for understanding PEP binding.

Conflicts of interest statement

The authors declare no conflicts of interest.

Acknowledgements

This work was supported by grants from FAPESP (BIOTA-BIOprospecTA program–Proc. 06/57122-7) and Millennium Institute, MCT/CNPq and FINEP/PRONALMO. MSP, DSS, and LAB are

research awardees from the National Council for Scientificand Technological Development (CNPq).

Appendix A. Supplementary data

Supplementary data associated with this article can be found, in the online version, at doi:10.1016/j.ijms.2010.06.002.

References

[1] World Health Organization, The W.H.O./IUATLD global project on anti-tuberculosis drug resistance surveillance. Anti-tuberculosis drug resistant in the world, report no. 2: prevalence and trends, World Health Organization. World Health Organization. Global Tuberculosis Control, Geneva, Switzerland, 2000.
[2] World Health Organization Report, WHO/CDS/TB/2001.287, Geneva, Switzerland, 2001.
[3] J.H. Pereira, F. Canduri, J.S. Oliveira, N.J.F. Silveira, L.A. Basso, M.S. Palma, W.F. de Azevedo Jr., D.S. Santos, Biochem. Biophys. Res. Commun. 312 (2003) 608.
[4] F. Roberts, C.W. Roberts, J.J. Johnson, D.E. Kyle, T. Krell, J.R. Coggins, G.H. Coombs, W.K. Milhous, S. Tzipori, D.J.P. Ferguson, D. Chakrabarti, R. McLeod, Nature 393 (1998) 801.
[5] K.M. Herrmann, L.M. Weaver, Annu. Rev. Plant. Physiol. Plant Mol. Biol. 50 (1999) 473.
[6] L.A. Basso, L.H.P. Da Silva, A.G. Fett-Neto, W.F. De Azevedo, I.S.M. Moreira, M.S. Palma, J.B. Calixto, S. Astolfi Filho, R.R. Santos, M. Soares, D.S. Santos, Mem. Inst. Oswaldo Cruz 100 (2005) 575.
[7] W.C. Stallings, S.S. Abdel-Meguid, L.W. Lim, H. Shieh, H.E. Dayringer, N.K. Leimgruber, R.A. Stegeman, K.S. Anderson, J.A. Sirorski, S.R. Padgette, G.M. Kishore, Proc. Natl. Acad. Sci. 88 (1991) 5046.
[8] T. Funke, H. Han, M.L. Healy-Friend, M. Fischer, E. Schöbrun, Proc. Natl. Acad. Sci. 103 (2006) 13010.
[9] M.R. Marques, A. Vaso, J.R. Ruggiero Neto, M.A. Fossey, J.S. Oliveira, L.A. Basso, D.S. Santos, W.F. Azevedo Junior, M.S. Palma, Biochemistry 47 (2008) 7509.
[10] M.R. Marques, J.H. Pereira, J.S. Oliveira, F. Canduri, L.A. Basso, D.S. Santos, W.F. Azevedo Junior, M.S. Palma, Curr. Drug Targets 8 (2007) 445.
[11] G.P. Bourenkov, G.S. Kachalova, N. Strizhov, M. Bruning, A. Vagin, H.D. Bartunik, Protein Data Bank, code: **2bjb**, 2006, http://www.rcsb.org/pdb/explore/explore.do?structureId=2BJB.
[12] H. Park, J.L. Hilsenbeck, H.J. Kim, W.A. Shuttleworth, Y.H. Park, J.N. Evans, C. Kang, Mol. Microbiol. 51 (2004) 963.
[13] G.A. McConkey, M.J. Rogers, T.F. Mc Cutchan, J. Biol. Chem. 272 (1997) 2046.
[14] E. Schönbrunn, S. Eschenburg, W.A. Shuttleworth, J.V. Schloss, N. Amrhein, J.N.S. Evans, W. Kabsch, Proc. Natl. Acad. Sci. U.S.A. 98 (2001) 1376.
[15] C.M. Dobson, Trends Biochem. Sci. 24 (1999) 329.
[16] F.H. Beijer, H. Kooijman, A.L. Spek, R.P. Sijbesma, E.W. Meijer, Angew. Chem. Int. Ed. 37 (1998) 75.
[17] J. Chen, W.E. Stites, Biochemistry 40 (2001) 14012.
[18] R. Liyanage, N. Devarapalli, L.M. Puckett, N.H. Phan, J. Gidden, W.E. Stites, J.O. Lay Jr., Int. J. Mass Spectrom. 287 (2009) (2009) 96.
[19] J.S. Shi, J.R. Koeppe, E.A. Komives, P. Paylor, J. Biol. Chem. 28 (2006) 12170.
[20] J.G. Williams, K.B. Tomer, C.E. Hioe, S. Zolla-Pazner, J. Am. Soc. Mass Spectrom. 17 (2006) 1560.
[21] A.J. Percy, G.W. Slysz, D.C. Schriemer, Anal. Chem. 81 (2009) 7900.
[22] X. Yan, D. Broderick, M.E. Leid, M.I. Schmerlik, M.L. Deizer, Biochemistry 43 (2004) 909.
[23] J.J. Englander, J.R. Rogero, S.W. Englander, Anal. Biochem. 147 (1985) 234.
[24] J.M. Hochrein, T.E. Wales, E.C. Lerner, A.P. Schiavone, T.E. Smithgall, J.R. Engen, Biochemistry 45 (2006) 7733.
[25] T.E. Wales, J.R. Engen, Mass Spectrom. Rev. 25 (2006) 158.
[26] J.S. Oliveira, C.A. Pinto, L.A. Basso, D.S. Santos, Protein Expr. Purif. 22 (2001) 430.
[27] J.S. Oliveira, M.A. Mendes, M.S. Palma, L.A. Basso, D.S. Santos, Protein Expr. Purif. 28 (2003) 287.
[28] C.N. Pace, F.L. Vajdos, F.G. Grimsley Fee, T. Gray, Protein Sci. 4 (1995) 2411.
[29] Z. Zhang, D.L. Smith, Protein Sci. 2 (1993) 522.
[30] P.L. Wintrode, F.L. Keneth, E. Vierling, J.B. Smith, D.L. Smith, Protein Sci. 42 (2003) 10667.
[31] Y. Tsuitsui, A. Gersheson, P.L. Wintrode, Biochemistry 45 (2006) 6561.
[32] Y. Deng, D.L. Smith, Biochemistry 37 (1998) 6256.
[33] M.Y. Kim, C.S. Maier, D.J. Reed, M.L. Deinzer, Protein Sci. 11 (2002) 1320.
[34] H.B. Uchôa, G.E. Jorge, N.J.F. Da Silveira, J.C. Camera Jr., F. Canduri, W.F. De Azevedo Jr., Biochem. Biophys. Res. Commun. 325 (2004) 1481.
[35] E. Schönbrunn, S. Eschenburg, W.A. Shuttleworth, J.V.N. Schloss, N. Amrhein, J.N.S. Evans, W. Kabsch, Proc. Natl. Acad. Sci. U.S.A. 98 (2001) 1376.